Supplement of

Rapid Iodine Oxoacids Nucleation Enhanced by Dimethylamine in Broad Marine Regions

Haotian Zu et al.

Correspondence to: Ling Liu (lingliu@bit.edu.cn) and Xiuhui Zhang (zhangxiuhui@bit.edu.cn)

Table of Contents

molecules cm^{-3}, $c(HIO_2) = 6.0 \times 10^4$ molecules cm^{-3}, $c(DMA) = 1.0 \times 10^6$ molecules cm^{-3}, $T = 268$ K, and CS = 1.0×10^{-4} s^{-1}. The clusters satisfying kinetically stable conditions ($\beta c/\Sigma\gamma > 1$, $n = 5$) in the simulated system and the corresponding $\beta c/\Sigma\gamma$ values are shown in red.

Table S5. The cartesian coordinates of the most stable clusters in the $(HIO_3)_x{\cdot}(HIO_2)_y{\cdot}(DMA)_z$ ($1 \leq x + y + z \leq 5$; $x + y \geq z$) system at the ωB97X-D/6-311++G(3df,3pd) (for H, C, N, and O atoms) + aug-cc-pVTZ-PP with ECP28MDF (for I atom) level of theory.

Table S6. The total number of proton transfer (N) and the number of proton transfer between different precursors in ternary clusters (n_1, n_2, n_3 represent the number of proton transfer between HIO_3 and DMA, HIO_3 and HIO_2, and HIO_2 and DMA, respectively).

Section S5: References

Section S1: The boundary clusters in the simulated system.

The boundary clusters are the smallest clusters outside the simulated system. Once the boundary clusters are formed, they tend to keep growing rather than evaporating into fragmented clusters. The boundary clusters in this work were set to be the clusters formed by the combination of kinetically stable clusters ($\beta c/\Sigma\gamma > 1$) with five molecules ($n = 5$) and the corresponding monomers at the concentration c. The clusters satisfying kinetically stable conditions ($\beta c/\Sigma\gamma > 1$, $n = 5$) in the simulated system and the corresponding $\beta c/\Sigma\gamma$ values can be seen from Tables S1-S4. The collision and total evaporation frequency of HIO_3-HIO_2/DMA clusters and pure-HIO_x ($x = 2, 3$) clusters presented in this work were adopted from the stable structures with the lowest Gibbs free energy of formation in previous studies (Rong et al., 2020; Zhang et al., 2022; Ning et al., 2022; Liu et al., 2023).

Section S2: The detailed description of HIO_3-HIO_2-DMA nucleation pathway under field conditions of Mace Head

The main cluster formation pathways, which contributed more than 5% to the total cluster formation rates, under field conditions of Mace Head are shown in Fig. 3. The nucleation pathways can be divided into three categories, such as the HIO_3-HIO_2 binary nucleation (53%), HIO_3-DMA binary nucleation (9%), and HIO_3-HIO_2-DMA ternary nucleation (38%). As can be seen in Fig. 3, although HIO_3-HIO_2 nucleation contributes most to the total cluster formation rates, DMA has a significant participation in the nucleation pathways. In ternary pathways, the molecules of HIO_3 and HIO_2/DMA will firstly combine to form binary cluster, then the binary cluster will combine with the third monomer or cluster that contains the third monomer to form ternary cluster, and finally the growth of cluster mainly proceeds by the sequential addition of HIO_3 monomer.

Section S3: The proportion of nucleation pathways under a wide range of oceanic atmospheric conditions with different ratios of [HIO_3] and [HIO_2]

The ratio of [HIO_3] to [HIO_2] is about 20 to 100 depending on the concentration of iodine vapor (He et al., 2021). Three concentration ratios of [HIO_3] and [HIO_2] were adopted to evaluate the impact of the concentration of iodine vapor on the proportion of nucleation pathways. The results were shown in Fig. S2 ([HIO_3] / [HIO_2] = 20), Fig. 4 ([HIO_3] / [HIO_2] = 50), and Fig. S3 ([HIO_3] / [HIO_2] = 100). Comparing the results under three conditions, when [DMA] is comparable to [HIO_2] (red dashed line in Fig. S2, Fig. 4, and Fig. S3), the ternary nucleation pathways have significant contributions that cannot be ignored and the changes of [HIO_3] / [HIO_2] will not affect this result. In addition, when the [HIO_3] / [HIO_2] increases ([HIO_2] reducing without changing [HIO_3]), the contributions of HIO_3-HIO_2 binary pathways are also reduced correspondingly. Besides, except for ternary nucleation, the contributions of HIO_3-DMA are significantly higher than those of HIO_3-HIO_2 when [DMA] is equal to [HIO_2] as shown in Fig. S4 marked by red dashed line. This indicates the important role of DMA in the nucleation of iodine oxoacids.

Section S4: Figures and Tables

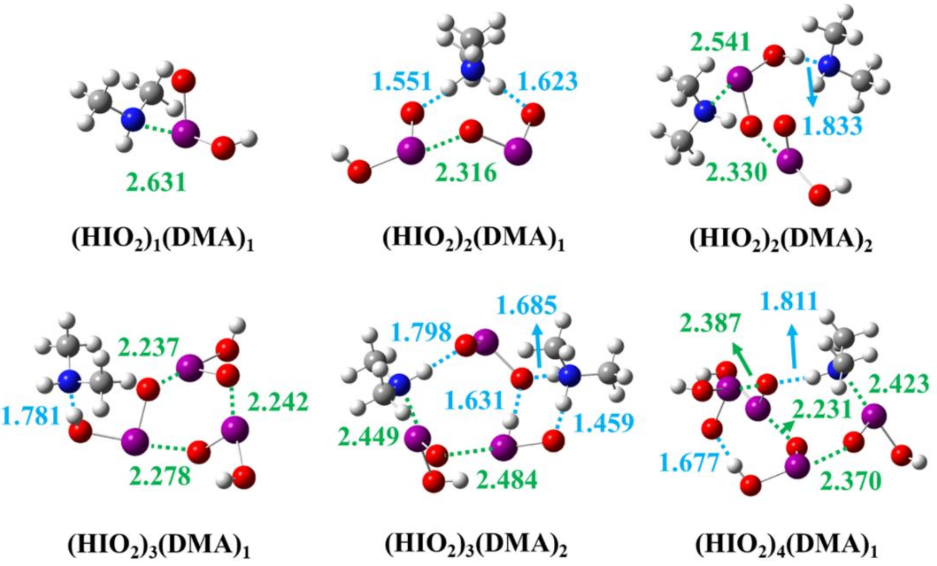

Figure S1. The most stable structures of HIO_2-DMA clusters identified at the ωB97X-D/6-311++G(3df,3pd) (for H, C, N, and O atoms) + aug-cc-pVTZ-PP with ECP28MDF (for I atom) level of theory. The white, grey, blue, red, and purple balls represent the H, C, N, O, and I atoms, respectively. The hydrogen bonds and halogen bonds are shown in blue and green dashed lines, respectively. The values of bond lengths are given in Å.

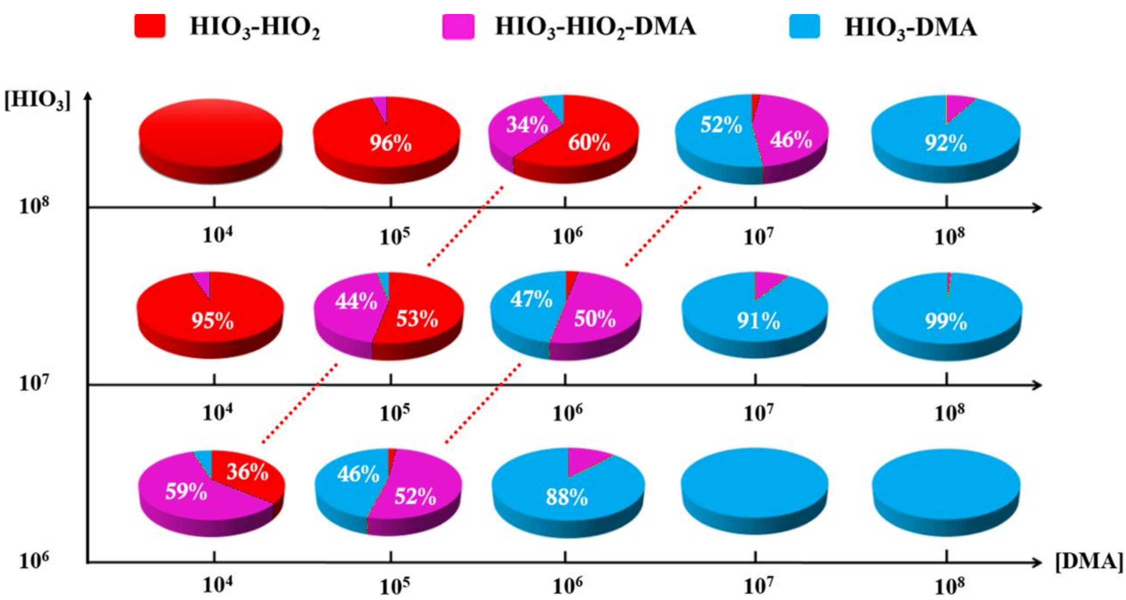

Figure S2. The contribution of main nucleation pathways at different concentrations of precursors. $[HIO_3] = 10^6 - 10^8$ molecules cm^{-3}, $[HIO_2] = 5.0 \times 10^4 - 5.0 \times 10^6$ molecules cm^{-3} and $[DMA] = 10^4 - 10^8$ molecules cm^{-3}. The simulated temperature and condensation sink are 283K and 2.0×10^{-3} s^{-1} as typical values for oceanic atmosphere. The contribution of HIO_3-HIO_2, HIO_3-HIO_2-DMA, and HIO_3-DMA are shown in red, purple, and blue, respectively. The red dashed line indicates the pie chart with significant contribution of ternary nucleation to the nucleation pathways.

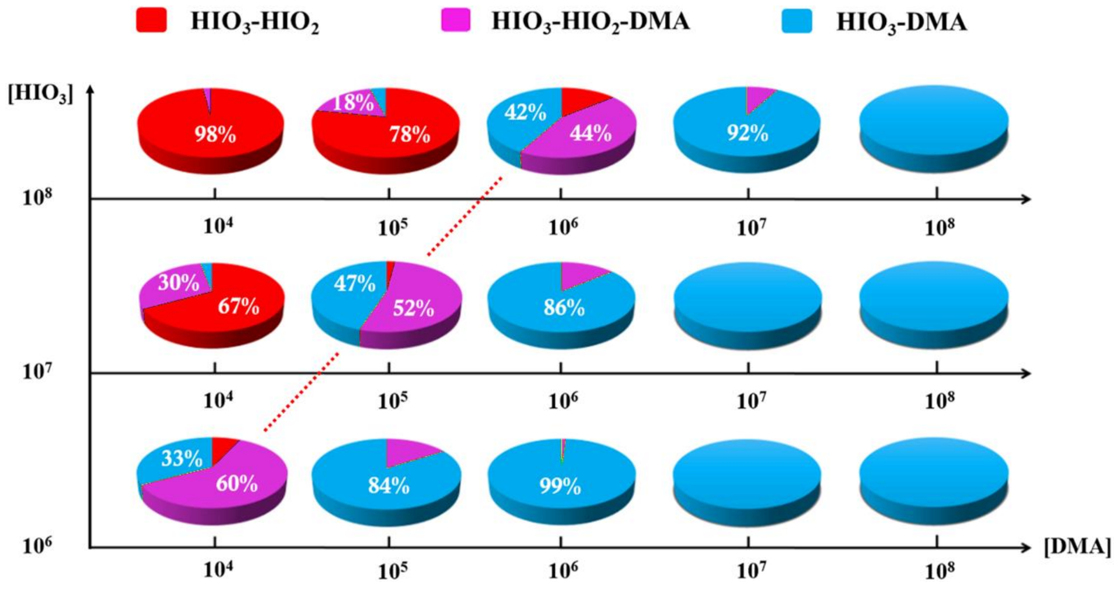

Figure S3. The contribution of main nucleation pathways at different concentrations of precursors. $[HIO_3]$ = 10^6 − 10^8 molecules cm^{-3}, $[HIO_2]$ = 10^4 − 10^6 molecules cm^{-3}, and [DMA] = 10^4 − 10^8 molecules cm^{-3}. The simulated temperature and condensation sink are 283K and 2.0 × 10^{-3} s^{-1} as typical values for oceanic atmosphere. The contribution of HIO_3-HIO_2, HIO_3-HIO_2-DMA, and HIO_3-DMA are shown in red, purple, and blue, respectively. The red dashed line indicates the pie chart with significant contribution of ternary nucleation to the nucleation pathways.

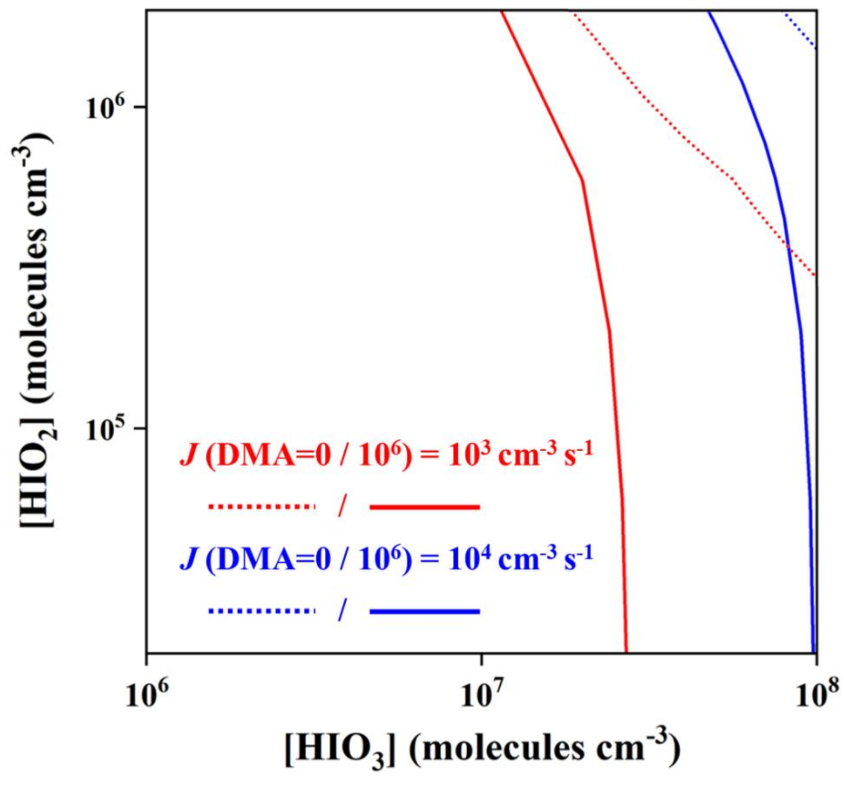

Figure S4. The isolines of formation rate (J, cm^{-3} s^{-1}) and the corresponding concentrations of precursors (molecules cm^{-3}) at T = 287 K and CS = 2.0×10^{-3} s^{-1}. The solid and dashed line indicates the formation rate with [DMA] = 10^6 molecules cm^{-3} and without DMA, respectively. The isoline of $J = 10^3$ and 10^4 cm^{-3} s^{-1} are shown in red and blue, respectively.

Table S1. The ratios of collision frequency between the clusters and monomer molecule at the concentration c to the total evaporation frequency of clusters in HIO_3-HIO_2-DMA system at $c(HIO_3) = 1.0 \times 10^8$, $c(HIO_2) = 2.0 \times 10^6$, $c(DMA) = 5.0 \times 10^5$, T = 283 K, and CS = 2.0×10^{-3} s^{-1}. The clusters satisfying kinetically stable conditions ($\beta c/\Sigma\gamma > 1$, $n = 5$) in the simulated system and the corresponding $\beta c/\Sigma\gamma$ values are shown in red.

Clusters	β	$\Sigma\gamma$	$\beta c(DMA)/\Sigma\gamma$	$\beta c(HIO_2)/\Sigma\gamma$	$\beta c(HIO_3)/\Sigma\gamma$
$(HIO_3)_2$	4.50×10^{-10}	2.63×10^{3}	8.54×10^{-8}	3.42×10^{-7}	1.71×10^{-5}
$(HIO_3)_3$	5.12×10^{-10}	9.47×10^{1}	2.70×10^{-6}	1.08×10^{-5}	5.41×10^{-4}
$(HIO_3)_4$	5.64×10^{-10}	4.03×10^{-6}	7.00×10^{1}	2.80×10^{2}	1.40×10^{4}
$(HIO_3)_5$	6.11×10^{-10}	2.13×10^{-4}	1.44×10^{0}	5.74×10^{0}	2.87×10^{2}
$(HIO_2)_2$	4.33×10^{-10}	1.11×10^{-4}	1.95×10^{0}	7.79×10^{0}	3.90×10^{2}
$(HIO_2)_3$	4.91×10^{-10}	2.82×10^{-7}	8.70×10^{2}	3.48×10^{3}	1.74×10^{5}
$(HIO_2)_4$	5.42×10^{-10}	7.42×10^{-6}	3.65×10^{1}	1.46×10^{2}	7.30×10^{3}
$(HIO_2)_5$	5.87×10^{-10}	5.81×10^{-4}	5.05×10^{-1}	2.02×10^{0}	1.01×10^{2}
$(HIO_3)_1(DMA)_1$	2.90×10^{-10}	5.40×10^{-3}	2.69×10^{-2}	1.08×10^{-1}	5.38×10^{0}
$(HIO_3)_2(DMA)_1$	5.17×10^{-10}	2.51×10^{-5}	1.03×10^{1}	4.12×10^{1}	2.06×10^{3}
$(HIO_3)_2(DMA)_2$	3.34×10^{-10}	2.20×10^{-6}	7.58×10^{1}	3.03×10^{2}	1.52×10^{4}
$(HIO_3)_3(DMA)_1$	5.67×10^{-10}	1.51×10^{0}	1.88×10^{-4}	7.51×10^{-4}	3.76×10^{-2}
$(HIO_3)_3(DMA)_2$	6.19×10^{-10}	3.44×10^{-6}	8.98×10^{1}	3.59×10^{2}	1.80×10^{4}
$(HIO_3)_4(DMA)_1$	6.15×10^{-10}	2.76×10^{-5}	1.11×10^{1}	4.46×10^{1}	2.23×10^{3}
$(HIO_2)_1(DMA)_1$	2.92×10^{-10}	7.52×10^{2}	1.94×10^{-7}	7.77×10^{-7}	3.89×10^{-5}
$(HIO_2)_2(DMA)_1$	5.08×10^{-10}	6.43×10^{-1}	3.95×10^{-4}	1.58×10^{-3}	7.91×10^{-2}
$(HIO_2)_2(DMA)_2$	3.30×10^{-10}	4.64×10^{5}	3.56×10^{-10}	1.42×10^{-9}	7.12×10^{-8}
$(HIO_2)_3(DMA)_1$	5.52×10^{-10}	1.57×10^{5}	1.76×10^{-9}	7.04×10^{-9}	3.52×10^{-7}
$(HIO_2)_3(DMA)_2$	3.44×10^{-10}	1.22×10^{-1}	1.41×10^{-3}	5.62×10^{-3}	2.81×10^{-1}
$(HIO_2)_4(DMA)_1$	5.96×10^{-10}	5.78×10^{0}	5.16×10^{-5}	2.06×10^{-4}	1.03×10^{-2}
$(HIO_3)_1(HIO_2)_1$	4.41×10^{-10}	1.19×10^{-4}	1.85×10^{0}	7.41×10^{0}	3.71×10^{2}
$(HIO_3)_1(HIO_2)_2$	4.96×10^{-10}	2.34×10^{-7}	1.06×10^{3}	4.23×10^{3}	2.12×10^{5}
$(HIO_3)_2(HIO_2)_1$	5.02×10^{-10}	2.37×10^{0}	1.06×10^{-4}	4.23×10^{-4}	2.12×10^{-2}
$(HIO_3)_3(HIO_2)_1$	5.58×10^{-10}	4.45×10^{-7}	6.27×10^{2}	2.51×10^{3}	1.25×10^{5}
$(HIO_3)_1(HIO_2)_3$	5.46×10^{-10}	1.68×10^{-2}	1.63×10^{-2}	6.51×10^{-2}	3.25×10^{0}
$(HIO_3)_2(HIO_2)_2$	5.50×10^{-10}	1.33×10^{-2}	2.07×10^{-2}	8.27×10^{-2}	4.14×10^{0}
$(HIO_3)_3(HIO_2)_2$	5.99×10^{-10}	2.95×10^{-4}	1.02×10^{0}	4.06×10^{0}	2.03×10^{2}
$(HIO_3)_2(HIO_2)_3$	5.96×10^{-10}	2.32×10^{-8}	1.29×10^{4}	5.14×10^{4}	2.57×10^{6}

$(HIO_3)_4(HIO_2)_1$	6.06×10^{-10}	1.53×10^{0}	1.98×10^{-4}	7.91×10^{-4}	3.95×10^{-2}
$(HIO_3)_1(HIO_2)_4$	5.93×10^{-10}	1.12×10^{-7}	2.65×10^{3}	1.06×10^{4}	5.30×10^{5}
$(HIO_3)_1(HIO_2)_1(DMA)_1$	5.15×10^{-10}	4.37×10^{-4}	5.90×10^{-1}	2.36×10^{0}	1.18×10^{2}
$(HIO_3)_1(HIO_2)_1(DMA)_2$	3.33×10^{-10}	9.38×10^{-2}	1.77×10^{-3}	7.10×10^{-3}	3.55×10^{-1}
$(HIO_3)_2(HIO_2)_1(DMA)_1$	5.67×10^{-10}	9.45×10^{-7}	3.00×10^{2}	1.20×10^{3}	6.00×10^{4}
$(HIO_3)_2(HIO_2)_1(DMA)_2$	3.51×10^{-10}	4.03×10^{-2}	4.35×10^{-3}	1.74×10^{-2}	8.70×10^{-1}
$(HIO_3)_1(HIO_2)_2(DMA)_1$	5.56×10^{-10}	7.01×10^{1}	3.97×10^{-6}	1.59×10^{-5}	7.93×10^{-4}
$(HIO_3)_1(HIO_2)_2(DMA)_2$	3.45×10^{-10}	1.46×10^{-2}	1.18×10^{-2}	4.73×10^{-2}	2.36×10^{0}
$(HIO_3)_3(HIO_2)_1(DMA)_1$	6.10×10^{-10}	7.37×10^{-4}	4.14×10^{-1}	1.65×10^{0}	8.27×10^{1}
$(HIO_3)_1(HIO_2)_3(DMA)_1$	6.04×10^{-10}	4.33×10^{-4}	6.98×10^{-1}	2.79×10^{0}	1.40×10^{2}
$(HIO_3)_2(HIO_2)_2(DMA)_1$	6.06×10^{-10}	2.42×10^{-7}	1.25×10^{3}	5.00×10^{3}	2.50×10^{5}

Table S2. The ratios of collision frequency between the clusters and monomer molecule at the concentration c to the total evaporation frequency of clusters in HIO_3-HIO_2-DMA system under field conditions of Mace Head at $c(HIO_3) = 1.0 \times 10^8$ molecules cm^{-3}, $c(HIO_2) = 2.0 \times 10^6$ molecules cm^{-3}, $c(DMA) = 5.0 \times 10^7$ molecules cm^{-3}, $T = 287$ K, and CS = 2.0×10^{-3} s^{-1}. The clusters satisfying kinetically stable conditions ($\beta c/\Sigma\gamma > 1$, $n = 5$) in the simulated system and the corresponding $\beta c/\Sigma\gamma$ values are shown in red.

Clusters	β	$\Sigma\gamma$	$\beta c(DMA)/\Sigma\gamma$	$\beta c(HIO_2)/\Sigma\gamma$	$\beta c(HIO_3)/\Sigma\gamma$
$(HIO_3)_2$	4.53×10^{-10}	4.14×10^{3}	5.48×10^{-6}	2.19×10^{-7}	1.10×10^{-5}
$(HIO_3)_3$	5.16×10^{-10}	1.63×10^{2}	1.58×10^{-4}	6.33×10^{-6}	3.16×10^{-4}
$(HIO_3)_4$	5.68×10^{-10}	8.80×10^{-6}	3.23×10^{3}	1.29×10^{2}	6.46×10^{3}
$(HIO_3)_5$	6.15×10^{-10}	4.40×10^{-4}	6.99×10^{1}	2.80×10^{0}	1.40×10^{2}
$(HIO_2)_2$	4.36×10^{-10}	2.29×10^{-4}	9.53×10^{1}	3.81×10^{0}	1.91×10^{2}
$(HIO_2)_3$	4.94×10^{-10}	6.27×10^{-7}	3.94×10^{4}	1.58×10^{3}	7.88×10^{4}
$(HIO_2)_4$	5.45×10^{-10}	1.63×10^{-5}	1.67×10^{3}	6.68×10^{1}	3.34×10^{3}
$(HIO_2)_5$	5.91×10^{-10}	1.14×10^{-3}	2.58×10^{1}	1.03×10^{0}	5.17×10^{1}
$(HIO_3)_1(DMA)_1$	2.92×10^{-10}	1.02×10^{-2}	1.44×10^{0}	5.76×10^{-2}	2.88×10^{0}
$(HIO_3)_2(DMA)_1$	5.21×10^{-10}	5.25×10^{-5}	4.96×10^{2}	1.98×10^{1}	9.92×10^{2}
$(HIO_3)_2(DMA)_2$	3.36×10^{-10}	4.64×10^{-6}	3.62×10^{3}	1.45×10^{2}	7.25×10^{3}
$(HIO_3)_3(DMA)_1$	5.70×10^{-10}	2.66×10^{0}	1.07×10^{-2}	4.29×10^{-4}	2.14×10^{-2}
$(HIO_3)_3(DMA)_2$	6.23×10^{-10}	7.95×10^{-6}	3.92×10^{3}	1.57×10^{2}	7.83×10^{3}
$(HIO_3)_4(DMA)_1$	6.19×10^{-10}	5.98×10^{-5}	5.18×10^{2}	2.07×10^{1}	1.04×10^{3}
$(HIO_2)_1(DMA)_1$	2.94×10^{-10}	1.20×10^{3}	1.23×10^{-5}	4.91×10^{-7}	2.45×10^{-5}

$(HIO_2)_2(DMA)_1$	5.12×10^{-10}	1.13×10^{0}	2.26×10^{-2}	9.04×10^{-4}	4.52×10^{-2}
$(HIO_2)_2(DMA)_2$	3.32×10^{-10}	6.91×10^{5}	2.41×10^{-8}	9.62×10^{-10}	4.81×10^{-8}
$(HIO_2)_3(DMA)_1$	5.56×10^{-10}	2.37×10^{5}	1.17×10^{-7}	4.69×10^{-9}	2.34×10^{-7}
$(HIO_2)_3(DMA)_2$	3.46×10^{-10}	2.29×10^{-1}	7.55×10^{-2}	3.02×10^{-3}	1.51×10^{-1}
$(HIO_2)_4(DMA)_1$	6.00×10^{-10}	9.91×10^{0}	3.03×10^{-3}	1.21×10^{-4}	6.06×10^{-3}
$(HIO_3)_1(HIO_2)_1$	4.44×10^{-10}	2.43×10^{-4}	9.14×10^{1}	3.66×10^{0}	1.83×10^{2}
$(HIO_3)_1(HIO_2)_2$	5.00×10^{-10}	5.33×10^{-7}	4.68×10^{4}	1.87×10^{3}	9.37×10^{4}
$(HIO_3)_2(HIO_2)_1$	5.05×10^{-10}	4.30×10^{0}	5.88×10^{-3}	2.35×10^{-4}	1.18×10^{-2}
$(HIO_3)_3(HIO_2)_1$	5.62×10^{-10}	9.84×10^{-7}	2.86×10^{4}	1.14×10^{3}	5.71×10^{4}
$(HIO_3)_1(HIO_2)_3$	5.50×10^{-10}	3.29×10^{-2}	8.37×10^{-1}	3.35×10^{-2}	1.67×10^{0}
$(HIO_3)_2(HIO_2)_2$	5.54×10^{-10}	2.55×10^{-2}	1.09×10^{0}	4.35×10^{-2}	2.17×10^{0}
$(HIO_3)_3(HIO_2)_2$	6.04×10^{-10}	6.29×10^{-4}	4.80×10^{1}	1.92×10^{0}	9.60×10^{1}
$(HIO_3)_2(HIO_2)_3$	6.01×10^{-10}	5.55×10^{-8}	5.41×10^{5}	2.17×10^{4}	1.08×10^{6}
$(HIO_3)_4(HIO_2)_1$	6.10×10^{-10}	2.80×10^{0}	1.09×10^{-2}	4.36×10^{-4}	2.18×10^{-2}
$(HIO_3)_1(HIO_2)_4$	5.97×10^{-10}	2.57×10^{-7}	1.16×10^{5}	4.65×10^{3}	2.32×10^{5}
$(HIO_3)_1(HIO_2)_1(DMA)_1$	5.19×10^{-10}	8.55×10^{-4}	3.03×10^{1}	1.21×10^{0}	6.07×10^{1}
$(HIO_3)_1(HIO_2)_1(DMA)_2$	3.35×10^{-10}	1.76×10^{-1}	9.50×10^{-2}	3.80×10^{-3}	1.90×10^{-1}
$(HIO_3)_2(HIO_2)_1(DMA)_1$	5.71×10^{-10}	2.20×10^{-6}	1.30×10^{4}	5.20×10^{2}	2.60×10^{4}
$(HIO_3)_2(HIO_2)_1(DMA)_2$	3.50×10^{-10}	7.65×10^{-2}	2.29×10^{-1}	9.15×10^{-3}	4.57×10^{-1}
$(HIO_3)_1(HIO_2)_2(DMA)_1$	5.60×10^{-10}	1.18×10^{2}	2.37×10^{-4}	9.49×10^{-6}	4.74×10^{-4}
$(HIO_3)_1(HIO_2)_2(DMA)_2$	3.47×10^{-10}	2.81×10^{-2}	6.19×10^{-1}	2.48×10^{-2}	1.24×10^{0}
$(HIO_3)_3(HIO_2)_1(DMA)_1$	6.15×10^{-10}	1.42×10^{-3}	2.16×10^{1}	8.64×10^{-1}	4.32×10^{1}
$(HIO_3)_1(HIO_2)_3(DMA)_1$	6.08×10^{-10}	8.47×10^{-4}	3.59×10^{1}	1.44×10^{0}	7.18×10^{1}
$(HIO_3)_2(HIO_2)_2(DMA)_1$	6.10×10^{-10}	5.45×10^{-7}	5.60×10^{4}	2.24×10^{3}	1.12×10^{5}

Table S3. The ratios of collision frequency between the clusters and monomer molecule at the concentration c to the total evaporation frequency of clusters in HIO_3-HIO_2-DMA system under field conditions of Zhejiang at $c(HIO_3) = 1.0\times10^{7}$ molecules cm^{-3}, $c(HIO_2) = 2.0\times10^{5}$ molecules cm^{-3}, $c(DMA) = 1.0\times10^{8}$ molecules cm^{-3}, $T = 290$ K, and CS = 1.0×10^{-2} s^{-1}. The clusters satisfying kinetically stable conditions ($\beta c/\Sigma\gamma > 1$, $n = 5$) in the simulated system and the corresponding $\beta c/\Sigma\gamma$ values are shown in red.

Clusters	β	$\Sigma\gamma$	$\beta c(DMA)/\Sigma\gamma$	$\beta c(HIO_2)/\Sigma\gamma$	$\beta c(HIO_3)/\Sigma\gamma$
$(HIO_3)_2$	4.58×10^{-10}	7.88×10^{3}	5.81×10^{-6}	1.16×10^{-8}	5.81×10^{-7}
$(HIO_3)_3$	5.21×10^{-10}	3.55×10^{2}	1.47×10^{-4}	2.94×10^{-7}	1.47×10^{-5}

$(HIO_3)_4$	5.74×10^{-10}	2.70×10^{-5}	2.12×10^{3}	4.25×10^{0}	2.12×10^{2}
$(HIO_3)_5$	6.21×10^{-10}	1.27×10^{-3}	4.89×10^{1}	9.78×10^{-2}	4.89×10^{0}
$(HIO_2)_2$	4.41×10^{-10}	6.35×10^{-4}	6.94×10^{1}	1.39×10^{-1}	6.94×10^{0}
$(HIO_2)_3$	4.99×10^{-10}	2.10×10^{-6}	2.38×10^{4}	4.76×10^{1}	2.38×10^{3}
$(HIO_2)_4$	5.51×10^{-10}	4.87×10^{-5}	1.13×10^{3}	2.26×10^{0}	1.13×10^{2}
$(HIO_2)_5$	5.97×10^{-10}	3.24×10^{-3}	1.84×10^{1}	3.69×10^{-2}	1.84×10^{0}
$(HIO_3)_1(DMA)_1$	2.95×10^{-10}	2.62×10^{-2}	1.13×10^{0}	2.25×10^{-3}	1.13×10^{-1}
$(HIO_3)_2(DMA)_1$	5.26×10^{-10}	1.50×10^{-4}	3.50×10^{2}	7.01×10^{-1}	3.50×10^{1}
$(HIO_3)_2(DMA)_2$	3.40×10^{-10}	1.32×10^{-5}	2.58×10^{3}	5.16×10^{0}	2.58×10^{2}
$(HIO_3)_3(DMA)_1$	5.76×10^{-10}	6.00×10^{0}	9.61×10^{-3}	1.92×10^{-5}	9.61×10^{-4}
$(HIO_3)_3(DMA)_2$	6.29×10^{-10}	2.68×10^{-5}	2.35×10^{3}	4.71×10^{0}	2.35×10^{2}
$(HIO_3)_4(DMA)_1$	6.26×10^{-10}	1.77×10^{-4}	3.54×10^{2}	7.07×10^{-1}	3.54×10^{1}
$(HIO_2)_1(DMA)_1$	2.97×10^{-10}	2.32×10^{3}	1.28×10^{-5}	2.57×10^{-8}	1.28×10^{-6}
$(HIO_2)_2(DMA)_1$	5.17×10^{-10}	2.62×10^{0}	1.97×10^{-2}	3.95×10^{-5}	1.97×10^{-3}
$(HIO_2)_2(DMA)_2$	3.36×10^{-10}	1.28×10^{6}	2.61×10^{-8}	5.23×10^{-11}	2.61×10^{-9}
$(HIO_2)_3(DMA)_1$	5.62×10^{-10}	4.21×10^{5}	1.34×10^{-7}	2.67×10^{-10}	1.34×10^{-8}
$(HIO_2)_3(DMA)_2$	3.50×10^{-10}	5.90×10^{-1}	5.94×10^{-2}	1.19×10^{-4}	5.94×10^{-3}
$(HIO_2)_4(DMA)_1$	6.07×10^{-10}	2.24×10^{1}	2.71×10^{-3}	5.42×10^{-6}	2.71×10^{-4}
$(HIO_3)_1(HIO_2)_1$	4.48×10^{-10}	6.83×10^{-4}	6.57×10^{1}	1.31×10^{-1}	6.57×10^{0}
$(HIO_3)_1(HIO_2)_2$	5.05×10^{-10}	1.79×10^{-6}	2.83×10^{4}	5.66×10^{1}	2.83×10^{3}
$(HIO_3)_2(HIO_2)_1$	5.11×10^{-10}	1.03×10^{1}	4.98×10^{-3}	9.96×10^{-6}	4.98×10^{-4}
$(HIO_3)_3(HIO_2)_1$	5.68×10^{-10}	3.11×10^{-6}	1.83×10^{4}	3.65×10^{1}	1.83×10^{3}
$(HIO_3)_1(HIO_2)_3$	5.56×10^{-10}	8.59×10^{-2}	6.47×10^{-1}	1.29×10^{-3}	6.47×10^{-2}
$(HIO_3)_2(HIO_2)_2$	5.60×10^{-10}	6.43×10^{-2}	8.71×10^{-1}	1.74×10^{-3}	8.71×10^{-2}
$(HIO_3)_3(HIO_2)_2$	6.10×10^{-10}	1.87×10^{-3}	3.27×10^{1}	6.53×10^{-2}	3.27×10^{0}
$(HIO_3)_2(HIO_2)_3$	6.07×10^{-10}	1.99×10^{-7}	3.05×10^{5}	6.11×10^{2}	3.05×10^{4}
$(HIO_3)_4(HIO_2)_1$	6.16×10^{-10}	6.65×10^{0}	9.27×10^{-3}	1.85×10^{-5}	9.27×10^{-4}
$(HIO_3)_1(HIO_2)_4$	6.04×10^{-10}	9.11×10^{-7}	6.63×10^{4}	1.33×10^{2}	6.63×10^{3}
$(HIO_3)_1(HIO_2)_1(DMA)_1$	5.24×10^{-10}	2.34×10^{-3}	2.24×10^{1}	4.49×10^{-2}	2.24×10^{0}
$(HIO_3)_1(HIO_2)_1(DMA)_2$	3.39×10^{-10}	4.33×10^{-1}	7.83×10^{-2}	1.57×10^{-4}	7.83×10^{-3}
$(HIO_3)_2(HIO_2)_1(DMA)_1$	5.77×10^{-10}	7.20×10^{-6}	8.02×10^{3}	1.60×10^{1}	8.02×10^{2}

$(HIO_3)_2(HIO_2)_1(DMA)_2$	3.57×10^{-10}	1.96×10^{-1}	1.82×10^{-1}	3.65×10^{-4}	1.82×10^{-2}
$(HIO_3)_1(HIO_2)_2(DMA)_1$	5.66×10^{-10}	2.45×10^{2}	2.31×10^{-4}	4.63×10^{-7}	2.31×10^{-5}
$(HIO_3)_1(HIO_2)_2(DMA)_2$	6.20×10^{-10}	7.37×10^{-2}	8.41×10^{-1}	1.68×10^{-3}	8.41×10^{-2}
$(HIO_3)_3(HIO_2)_1(DMA)_1$	6.21×10^{-10}	3.75×10^{-3}	1.66×10^{1}	3.31×10^{-2}	1.66×10^{0}
$(HIO_3)_1(HIO_2)_3(DMA)_1$	6.15×10^{-10}	2.20×10^{-3}	2.79×10^{1}	5.58×10^{-2}	2.79×10^{0}
$(HIO_3)_2(HIO_2)_2(DMA)_1$	6.16×10^{-10}	1.76×10^{-6}	3.50×10^{4}	7.00×10^{1}	3.50×10^{3}

Table S4. The ratios of collision frequency between the clusters and monomer molecule at the concentration c to the total evaporation frequency of clusters in HIO_3-HIO_2-DMA system under field conditions of Aboa at $c(HIO_3) = 3.0 \times 10^6$ molecules cm^{-3}, $c(HIO_2) = 6.0 \times 10^4$ molecules cm^{-3}, $c(DMA) = 1.0 \times 10^6$ molecules cm^{-3}, $T = 268$ K, and CS = 1.0×10^{-4} s^{-1}. The clusters satisfying kinetically stable conditions ($\beta c/\Sigma\gamma > 1$, $n = 5$) in the simulated system and the corresponding $\beta c/\Sigma\gamma$ values are shown in red.

Clusters	β	$\Sigma\gamma$	$\beta c(DMA)/\Sigma\gamma$	$\beta c(HIO_2)/\Sigma\gamma$	$\beta c(HIO_3)/\Sigma\gamma$
$(HIO_3)_2$	4.38×10^{-10}	4.32×10^{2}	1.01×10^{-6}	6.08×10^{-8}	3.04×10^{-6}
$(HIO_3)_3$	4.98×10^{-10}	1.10×10^{1}	4.51×10^{-5}	2.71×10^{-6}	1.35×10^{-4}
$(HIO_3)_4$	5.49×10^{-10}	1.71×10^{-7}	3.21×10^{3}	1.93×10^{2}	9.64×10^{3}
$(HIO_3)_5$	5.94×10^{-10}	1.16×10^{-5}	5.10×10^{1}	3.06×10^{0}	1.53×10^{2}
$(HIO_2)_2$	4.22×10^{-10}	6.31×10^{-6}	6.68×10^{1}	4.01×10^{0}	2.01×10^{2}
$(HIO_2)_3$	4.78×10^{-10}	1.04×10^{-8}	4.60×10^{4}	2.76×10^{3}	1.38×10^{5}
$(HIO_2)_4$	5.27×10^{-10}	3.39×10^{-7}	1.56×10^{3}	9.34×10^{1}	4.67×10^{3}
$(HIO_2)_5$	5.71×10^{-10}	3.37×10^{-5}	1.69×10^{1}	1.02×10^{0}	5.08×10^{1}
$(HIO_3)_1(DMA)_1$	2.83×10^{-10}	3.99×10^{-4}	7.07×10^{-1}	4.24×10^{-2}	2.12×10^{0}
$(HIO_3)_2(DMA)_1$	5.03×10^{-10}	1.34×10^{-6}	3.74×10^{2}	2.25×10^{1}	1.12×10^{3}
$(HIO_3)_2(DMA)_2$	3.25×10^{-10}	1.16×10^{-7}	2.80×10^{3}	1.68×10^{2}	8.41×10^{3}
$(HIO_3)_3(DMA)_1$	5.51×10^{-10}	1.52×10^{-1}	3.63×10^{-3}	2.18×10^{-4}	1.09×10^{-2}
$(HIO_3)_3(DMA)_2$	6.02×10^{-10}	1.19×10^{-7}	5.05×10^{3}	3.03×10^{2}	1.52×10^{4}
$(HIO_3)_4(DMA)_1$	5.98×10^{-10}	1.35×10^{-6}	4.44×10^{2}	2.67×10^{1}	1.33×10^{3}
$(HIO_2)_1(DMA)_1$	2.84×10^{-10}	1.19×10^{2}	2.39×10^{-6}	1.44×10^{-7}	7.18×10^{-6}
$(HIO_2)_2(DMA)_1$	4.95×10^{-10}	6.41×10^{-2}	7.72×10^{-3}	4.63×10^{-4}	2.32×10^{-2}
$(HIO_2)_2(DMA)_2$	3.21×10^{-10}	8.55×10^{4}	3.76×10^{-9}	2.25×10^{-10}	1.13×10^{-8}
$(HIO_2)_3(DMA)_1$	5.37×10^{-10}	3.05×10^{4}	1.76×10^{-8}	1.06×10^{-9}	5.28×10^{-8}
$(HIO_2)_3(DMA)_2$	3.35×10^{-10}	9.44×10^{-3}	3.55×10^{-2}	2.13×10^{-3}	1.06×10^{-1}
$(HIO_2)_4(DMA)_1$	5.80×10^{-10}	6.32×10^{-1}	9.19×10^{-4}	5.51×10^{-5}	2.76×10^{-3}

$(HIO_3)_1(HIO_2)_1$	4.29×10^{-10}	6.63×10^{-6}	6.47×10^{1}	3.88×10^{0}	1.94×10^{2}
$(HIO_3)_1(HIO_2)_2$	4.83×10^{-10}	8.29×10^{-9}	5.83×10^{4}	3.50×10^{3}	1.75×10^{5}
$(HIO_3)_2(HIO_2)_1$	4.88×10^{-10}	2.13×10^{-1}	2.30×10^{-3}	1.38×10^{-4}	6.89×10^{-3}
$(HIO_3)_3(HIO_2)_1$	5.43×10^{-10}	1.87×10^{-8}	2.91×10^{4}	1.74×10^{3}	8.72×10^{4}
$(HIO_3)_1(HIO_2)_3$	5.31×10^{-10}	1.15×10^{-3}	4.62×10^{-1}	2.77×10^{-2}	1.39×10^{0}
$(HIO_3)_2(HIO_2)_2$	5.36×10^{-10}	9.95×10^{-4}	5.38×10^{-1}	3.23×10^{-2}	1.61×10^{0}
$(HIO_3)_3(HIO_2)_2$	5.83×10^{-10}	1.50×10^{-5}	3.90×10^{1}	2.34×10^{0}	1.17×10^{2}
$(HIO_3)_2(HIO_2)_3$	5.80×10^{-10}	6.94×10^{-10}	8.36×10^{5}	5.02×10^{4}	2.51×10^{6}
$(HIO_3)_4(HIO_2)_1$	5.90×10^{-10}	1.35×10^{-1}	4.36×10^{-3}	2.61×10^{-4}	1.31×10^{-2}
$(HIO_3)_1(HIO_2)_4$	5.77×10^{-10}	3.53×10^{-9}	1.64×10^{5}	9.82×10^{3}	4.91×10^{5}
$(HIO_3)_1(HIO_2)_1(DMA)_1$	5.01×10^{-10}	2.82×10^{-5}	1.78×10^{1}	1.07×10^{0}	5.33×10^{1}
$(HIO_3)_1(HIO_2)_1(DMA)_2$	3.26×10^{-10}	7.72×10^{-3}	4.22×10^{-2}	2.53×10^{-3}	1.27×10^{-1}
$(HIO_3)_2(HIO_2)_1(DMA)_1$	5.52×10^{-10}	3.40×10^{-8}	1.62×10^{4}	9.73×10^{2}	4.87×10^{4}
$(HIO_3)_2(HIO_2)_1(DMA)_2$	3.38×10^{-10}	3.01×10^{-3}	1.12×10^{-1}	6.75×10^{-3}	3.37×10^{-1}
$(HIO_3)_1(HIO_2)_2(DMA)_1$	5.41×10^{-10}	9.02×10^{0}	6.00×10^{-5}	3.60×10^{-6}	1.80×10^{-4}
$(HIO_3)_1(HIO_2)_2(DMA)_2$	5.93×10^{-10}	1.03×10^{-3}	5.77×10^{-1}	3.46×10^{-2}	1.73×10^{0}
$(HIO_3)_3(HIO_2)_1(DMA)_1$	5.94×10^{-10}	4.93×10^{-5}	1.20×10^{1}	7.22×10^{-1}	3.61×10^{1}
$(HIO_3)_1(HIO_2)_3(DMA)_1$	5.88×10^{-10}	2.99×10^{-5}	1.96×10^{1}	1.18×10^{0}	5.89×10^{1}
$(HIO_3)_2(HIO_2)_2(DMA)_1$	5.89×10^{-10}	9.06×10^{-9}	6.50×10^{4}	3.90×10^{3}	1.95×10^{5}

Table S5. The cartesian coordinates of the most stable clusters in the $(HIO_3)_x\cdot(HIO_2)_y\cdot(DMA)_z$ ($1 \leq x + y + z \leq 5$; $x + y \geq z$) system at the ωB97X-D/6-311++G(3df,3pd) (for H, C, N, and O atoms) + aug-cc-pVTZ-PP with ECP28MDF (for I atom) level of theory.

$(HIO_2)_1(DMA)_1$	X	Y	Z
I	0.658571	-0.020269	-0.190744
O	0.187400	0.169519	1.564530
O	2.645047	-0.099895	-0.022326
H	2.965606	0.766330	0.240732
N	-1.948511	-0.053029	-0.540662
H	-2.207771	-0.152829	-1.513594
C	-2.449431	1.217424	-0.021533
H	-2.028979	1.370161	0.972172
H	-2.121540	2.031231	-0.666460
H	-3.542177	1.232301	0.043851
C	-2.439451	-1.198138	0.222855
H	-2.105616	-2.122357	-0.245965

H	-2.018438	-1.145113	1.226754
H	-3.532070	-1.206991	0.290983

$(HIO_2)_2(DMA)_1$	X	Y	Z
I	1.734427	-1.241216	-0.097416
O	0.273177	-0.658953	0.957135
O	2.607205	0.339725	-0.515932
H	1.647693	1.626316	-0.270023
I	-1.853283	-0.347197	0.093926
O	-1.434824	1.400392	-0.349535
O	-3.725856	-0.272920	-0.604296
H	-4.255105	0.283394	-0.028400
N	0.964943	2.389075	-0.018593
H	0.002429	1.953974	-0.164307
C	1.129874	3.541499	-0.910760
H	2.121769	3.970674	-0.782479
H	1.007399	3.208216	-1.937633
H	0.374069	4.290226	-0.683111
C	1.112484	2.690935	1.411597
H	0.969604	1.765149	1.963293
H	2.107226	3.088017	1.604058
H	0.357916	3.415884	1.709721

$(HIO_2)_2(DMA)_2$	X	Y	Z
I	-1.658755	0.460005	-0.467585
O	-0.314217	-0.489985	-1.344284
O	-1.277141	2.196062	-1.274214
H	-0.542544	2.531125	-0.695740
I	1.718889	-0.942050	-0.299461
O	0.903723	-0.398470	1.269363
O	3.464459	-1.515882	0.497269
H	3.966036	-0.738487	0.751943
N	-1.792827	-1.694265	0.873085
H	-0.854216	-1.540427	1.248524
C	-1.847742	-2.941638	0.122425
H	-2.831838	-3.046756	-0.335402
H	-1.100638	-2.914435	-0.667617
H	-1.666918	-3.812247	0.760758
C	-2.774948	-1.607961	1.942704
H	-2.666056	-0.655321	2.461378
H	-3.779753	-1.665620	1.521612
H	-2.663915	-2.412799	2.675797
N	0.739315	2.644537	0.609266
H	0.855898	1.692045	0.957495
C	0.272453	3.487898	1.698538
H	0.033711	4.482070	1.317388
H	-0.634017	3.061985	2.127386

H	1.015274	3.598599	2.498619
C	1.995945	3.108408	0.041421
H	2.319336	2.419626	-0.737957
H	1.854118	4.090210	-0.412997
H	2.794145	3.192886	0.790181

$(HIO_2)_3(DMA)_1$	**X**	**Y**	**Z**
I	-1.288793	-0.614419	-1.150838
O	-0.912311	0.679673	0.183622
O	-3.156270	-0.055064	-1.309194
H	-3.592690	-0.193879	-0.427498
I	1.838934	-1.439461	0.517583
O	0.947791	-1.044224	-1.087961
O	1.936499	-3.400347	0.149404
H	1.099429	-3.814144	0.370319
I	0.864578	2.024041	-0.019902
O	1.814685	0.753979	0.982315
O	2.458268	3.205825	-0.228735
H	2.690215	3.592930	0.618639
N	-4.155644	-0.177217	1.262100
H	-5.117068	-0.482339	1.328407
C	-4.065103	1.240158	1.596674
H	-3.045823	1.575056	1.405321
H	-4.735806	1.811815	0.957515
H	-4.311017	1.443129	2.645863
C	-3.320454	-1.002677	2.126185
H	-3.447213	-2.053378	1.868517
H	-2.275363	-0.729647	1.972391
H	-3.551189	-0.871174	3.190396

$(HIO_2)_3(DMA)_2$	**X**	**Y**	**Z**
I	0.718367	-2.101422	0.405252
O	2.558331	-2.411959	0.315507
O	0.479007	-1.393225	-1.390836
H	0.864683	-0.469335	-1.390017
I	0.831779	2.429419	-0.488019
O	0.436562	1.838567	1.225399
O	1.669167	0.945507	-1.288459
H	3.031043	0.381488	-0.471691
I	-2.468416	-0.336251	-0.532182
O	-1.720609	-1.652224	0.537839
O	-2.576665	-1.470118	-2.160190
H	-1.664950	-1.647590	-2.419862
N	-2.269814	1.079736	1.455589
H	-1.252993	1.268640	1.454065
C	-2.658427	0.416303	2.694456
H	-3.731619	0.220797	2.684987

H	-2.136423	-0.534392	2.764723
H	-2.421547	1.032578	3.566605
C	-2.967930	2.338428	1.231894
H	-2.625908	2.784965	0.297140
H	-4.042619	2.162535	1.161743
H	-2.783504	3.053586	2.038041
N	3.692322	-0.118706	0.168140
H	3.243477	-1.124303	0.270678
C	3.676826	0.556637	1.473589
H	4.177681	1.521490	1.400426
H	2.640527	0.716254	1.770510
H	4.185809	-0.063670	2.208664
C	5.019289	-0.244440	-0.440521
H	4.918238	-0.748573	-1.397984
H	5.462443	0.739011	-0.590528
H	5.661506	-0.837180	0.208086

$(HIO_2)_4(DMA)_1$	X	Y	Z
I	-0.775912	1.312470	-1.642183
O	-1.002013	1.141753	0.215034
O	-1.976055	2.903948	-1.765655
H	-2.886062	2.602173	-1.822264
I	0.394235	-1.941535	-0.550373
O	0.711552	-0.344403	-1.501518
O	-1.194610	-2.476698	-1.530316
H	-1.950227	-1.959687	-1.144707
I	3.226659	0.292934	0.452531
O	2.287316	-1.290244	0.717225
O	4.669929	-0.536051	-0.641935
H	5.196001	-1.122115	-0.092325
I	-2.861345	-0.043979	1.128917
O	-3.036581	-0.844767	-0.520275
O	-4.258183	-1.081694	2.100344
H	-5.124293	-0.817468	1.780864
N	1.410289	1.310798	1.692552
H	0.573417	1.164400	1.111121
C	1.641033	2.748482	1.800094
H	2.556730	2.937117	2.363101
H	1.741770	3.179270	0.804294
H	0.811727	3.247701	2.305982
C	1.196018	0.664006	2.985346
H	1.042183	-0.400607	2.826951
H	2.074263	0.803247	3.616434
H	0.326519	1.086599	3.495564

$(HIO_3)_1(HIO_2)_1(DMA)_1$	X	Y	Z
I	2.316688	-0.503442	-0.206126

O	1.554964	-1.284788	1.371024
O	2.056555	1.305175	0.022866
H	0.567314	1.928605	0.052495
N	-0.329147	2.475749	0.165587
H	-1.064453	1.791422	0.473196
C	-0.724339	3.019663	-1.143411
H	0.050378	3.692654	-1.504422
H	-0.848141	2.183503	-1.826794
H	-1.664721	3.557538	-1.040815
C	-0.134557	3.489150	1.212355
H	0.172394	2.990503	2.127328
H	0.639710	4.187367	0.902679
H	-1.068271	4.021299	1.380638
I	-2.037764	-0.796127	-0.112645
O	-2.269014	0.715891	0.861029
O	-0.992352	-0.216395	-1.454518
O	-0.936709	-1.818050	0.895461
H	0.582676	-1.473509	1.190872

$(HIO_3)_1(HIO_2)_1(DMA)_2$	**X**	**Y**	**Z**
I	-2.237208	-0.193672	-0.270067
O	-1.599683	0.722399	1.212037
O	-3.312564	1.374459	-0.953898
H	-4.047101	1.536146	-0.357827
N	0.249304	2.468104	0.509521
H	-0.451917	1.720292	0.809376
C	-0.028847	2.814372	-0.896180
H	0.584982	3.663491	-1.191092
H	0.223718	1.949412	-1.507101
H	-1.085315	3.052619	-1.006478
C	0.153496	3.599210	1.439785
H	0.345442	3.242908	2.448246
H	0.889042	4.355792	1.174300
H	-0.846456	4.024892	1.389297
N	-0.884171	-1.975303	0.521170
H	0.042282	-1.560366	0.695305
C	-0.725104	-2.987014	-0.519658
H	-1.698304	-3.402389	-0.789346
H	-0.268415	-2.523459	-1.393047
H	-0.082298	-3.800582	-0.176486
C	-1.381332	-2.509318	1.787294
H	-1.481377	-1.691033	2.497194
H	-2.355161	-2.976193	1.635501
H	-0.688811	-3.251664	2.190482
I	2.595470	-0.364202	-0.249910
O	1.840992	-1.398348	1.020775
O	1.274629	-0.204560	-1.464410

O	2.679538	1.286177	0.497475
H	1.203311	2.033364	0.562316

$(HIO_3)_2(HIO_2)_1(DMA)_1$	X	Y	Z
N	0.284414	2.278090	0.392016
H	-0.733907	2.117166	0.587880
C	0.392173	2.435112	-1.077689
H	1.437420	2.558928	-1.344379
H	-0.021210	1.546152	-1.547184
H	-0.196808	3.304029	-1.362721
C	0.798228	3.436594	1.150002
H	0.664680	3.247940	2.211645
H	1.854815	3.554692	0.923008
H	0.242773	4.324328	0.857117
I	3.208060	0.068202	-0.045293
O	1.938410	-0.567373	-1.191455
O	3.458041	1.768710	-0.532297
O	2.183240	0.210282	1.451831
H	0.811349	1.452675	0.712039
I	-3.243375	0.558139	-0.143597
O	-2.384788	2.047421	0.411286
O	-2.074171	-0.193428	-1.312883
O	-3.155319	-0.547321	1.277211
H	-2.191403	-1.897047	0.999753
O	-1.589641	-2.568892	0.584998
I	-0.126109	-1.603976	-0.200890
O	1.135231	-2.391962	1.046974
H	1.466445	-1.630529	1.557886

$(HIO_3)_2(HIO_2)_1(DMA)_2$	X	Y	Z
I	3.280965	0.691446	-0.497634
O	3.117687	-1.068087	0.076504
O	2.072102	1.634054	0.600972
H	1.450785	0.529791	1.754418
N	1.108589	-0.149032	2.473223
H	0.608183	-0.897917	1.936657
C	0.154890	0.517935	3.374666
H	0.639678	1.372225	3.843097
H	-0.711795	0.828958	2.794939
H	-0.164495	-0.187212	4.138857
C	2.273099	-0.745646	3.148710
H	2.911148	-1.189923	2.388317
H	2.813194	0.032049	3.685418
H	1.930071	-1.505669	3.846938
N	-0.207652	2.466714	-0.611746
H	0.594381	1.970775	-0.147557
C	-0.689235	3.538763	0.271398

H	-1.486991	4.082445	-0.229264
H	-1.085253	3.079988	1.173659
H	0.135902	4.205958	0.510390
C	0.242148	2.924661	-1.934854
H	0.578694	2.055701	-2.493723
H	-0.590877	3.395062	-2.452067
H	1.057865	3.634596	-1.814091
I	-0.285846	-1.939108	-0.647979
O	-0.175966	-2.112279	1.136539
O	0.066701	-0.217427	-0.971896
O	1.431354	-2.620322	-1.107527
H	2.135321	-2.022225	-0.682084
I	-3.331281	0.339395	0.070510
O	-2.638433	-1.283993	-0.386276
O	-2.414133	0.869146	1.520448
O	-2.735448	1.463491	-1.206035
H	-0.982106	1.798840	-0.765099

$(HIO_3)_1(HIO_2)_2(DMA)_1$	**X**	**Y**	**Z**
I	2.427309	-0.247135	-0.556539
O	1.762962	1.046571	0.611066
O	2.966225	1.066267	-1.952035
H	2.186205	1.330196	-2.447773
I	-0.344297	1.979106	0.482502
O	-0.669179	0.702779	-0.868938
O	-2.123879	2.789484	0.332162
H	-2.741931	2.078173	0.572016
N	1.736738	-1.757810	1.167199
H	0.716877	-1.649841	1.099037
C	2.207284	-1.398037	2.502026
H	3.291294	-1.505914	2.549677
H	1.948393	-0.361865	2.702157
H	1.756495	-2.041951	3.260825
C	2.070644	-3.124875	0.778617
H	1.609986	-3.347101	-0.182963
H	3.153234	-3.237429	0.698270
H	1.698940	-3.846313	1.509033
I	-2.144800	-0.942144	-0.476218
O	-2.983318	0.138951	0.679473
O	-0.953977	-1.843297	0.515219
O	-3.533649	-2.330247	-0.430875
H	-3.890900	-2.400696	0.460386

$(HIO_3)_1(HIO_2)_2(DMA)_2$	**X**	**Y**	**Z**
I	2.373448	1.100392	0.225742
O	0.699414	0.192903	0.430804
O	1.357040	2.795669	0.359926

H	0.745498	2.786285	-0.430274
I	1.278152	-1.932200	-0.091764
O	2.939794	-1.008930	0.205477
O	2.235361	-3.644192	-0.391237
H	2.633333	-3.642809	-1.264695
N	-1.203121	1.544661	1.842851
H	-0.515466	1.203615	1.141771
C	-0.499663	1.645645	3.130005
H	-1.206116	1.921399	3.909383
H	-0.056346	0.680173	3.357288
H	0.280423	2.399242	3.046587
C	-1.826910	2.798069	1.392865
H	-2.362917	2.591558	0.469990
H	-2.522490	3.144660	2.154303
H	-1.049138	3.539477	1.226131
N	-0.386012	2.460116	-1.758226
H	-1.089764	1.825560	-1.382022
C	0.267176	1.765580	-2.860639
H	1.126281	2.341628	-3.209196
H	0.617302	0.793219	-2.516566
H	-0.407484	1.603917	-3.709891
C	-1.037153	3.686812	-2.191555
H	-1.548342	4.151001	-1.348435
H	-0.288978	4.391151	-2.558868
H	-1.770533	3.518084	-2.989218
I	-2.951638	-0.937131	-0.167158
O	-2.600037	0.649565	-0.949305
O	-1.476024	-1.934404	-0.429133
O	-2.912769	-0.510528	1.596131
H	-1.922235	0.774867	1.864539

$(HIO_3)_1(HIO_2)_3(DMA)_1$	**X**	**Y**	**Z**
I	-0.460929	-2.091419	-0.868175
O	-1.144462	-0.780118	-2.048324
O	1.027738	-2.574785	-2.004876
H	1.770430	-1.966456	-1.773982
I	-1.830808	1.196469	-1.509716
O	-0.919027	1.036372	0.137942
O	-2.367465	3.092268	-1.059574
H	-3.154168	3.087060	-0.510673
I	-1.799370	-0.230667	1.875917
O	-2.280762	-1.437507	0.537074
O	-2.359382	-1.384544	3.386965
H	-3.317479	-1.447572	3.404450
N	1.304111	2.633475	0.368844
H	0.625995	1.864823	0.207564
C	1.002312	3.736106	-0.559193

H	1.647891	4.582055	-0.335280
H	1.192785	3.396615	-1.574074
H	-0.044619	4.016987	-0.459427
C	1.208038	2.989789	1.793701
H	1.425727	2.094375	2.371056
H	1.935421	3.765435	2.021172
H	0.202913	3.348194	2.006955
I	3.489001	-0.220361	0.339687
O	2.036306	-0.223022	1.401115
O	2.904359	-0.838608	-1.249260
O	3.723246	1.555101	0.032483
H	2.271436	2.244384	0.186135

$(HIO_3)_3(HIO_2)_1(DMA)_1$	X	Y	Z
I	2.685796	0.056689	0.838679
O	0.798717	-0.054666	0.498709
O	2.344151	1.201103	2.390284
H	1.975802	2.023245	2.013715
N	-0.747757	-1.347963	2.439159
H	-0.135390	-0.981997	1.690805
C	-0.151742	-2.565751	3.011840
H	-0.837290	-2.984799	3.744504
H	0.020438	-3.272353	2.205487
H	0.790475	-2.314324	3.494549
C	-0.981171	-0.257010	3.405231
H	-1.514404	0.539883	2.890679
H	-1.587008	-0.632154	4.226535
H	-0.024372	0.106259	3.774409
I	0.756176	-1.555458	-1.329889
O	0.262125	-2.811950	-0.178887
O	2.548717	-1.351463	-0.928638
O	1.116249	-2.746289	-2.818023
H	1.447745	-3.585497	-2.478151
I	-3.217178	-0.292159	-0.061801
O	-2.810373	1.145473	0.937312
O	-1.744852	-0.429891	-1.115129
O	-3.061754	-1.668212	1.100404
H	-1.653799	-1.576276	1.953302
I	-0.072887	2.199549	-0.490783
O	0.875218	1.616003	-1.885053
O	1.133340	2.948513	0.600677
O	-0.760280	3.811653	-1.326219
H	-0.111550	4.111278	-1.974796

$(HIO_3)_2(HIO_2)_2(DMA)_1$	X	Y	Z
I	2.605369	-1.264764	0.260061
O	1.212760	-0.075171	0.744079

O	3.945182	-0.163505	1.191982
H	3.901435	0.713056	0.771251
I	-0.726983	-1.882105	-1.050222
O	0.967684	-2.577354	-0.625093
O	-0.295622	-0.927192	-2.642126
H	0.088935	-0.051045	-2.363824
N	-0.661456	-0.404327	2.639736
H	0.020691	-0.333937	1.846005
C	-0.344392	-1.607310	3.424972
H	-1.076643	-1.727035	4.219797
H	-0.373835	-2.473644	2.768827
H	0.652095	-1.509243	3.849980
C	-0.595790	0.855351	3.400783
H	-0.881491	1.662545	2.730809
H	-1.290005	0.810191	4.236637
H	0.418677	1.006771	3.762830
I	1.137208	2.059389	-0.312679
O	0.892526	1.268264	-1.900228
O	2.917654	2.108077	-0.158940
O	0.924365	3.888097	-0.953090
H	1.548051	4.045522	-1.670827
I	-3.251686	0.593137	0.118394
O	-1.695830	1.498335	0.230203
O	-3.025921	-0.612035	-1.210207
O	-3.167745	-0.422847	1.619448
H	-1.624195	-0.478335	2.223226

Table S6. The total number of proton transfer (*N*) and the number of proton transfer between different precursors in ternary clusters (n_1, n_2, n_3 represent the number of proton transfer between HIO_3 and DMA, HIO_3 and HIO_2, and HIO_2 and DMA, respectively).

Clusters	N	n_1	n_2	n_3
$(HIO_3)_1(HIO_2)_1(DMA)_1$	1	1	0	0
$(HIO_3)_1(HIO_2)_1(DMA)_2$	1	1	0	0
$(HIO_3)_2(HIO_2)_1(DMA)_1$	2	1	1	0
$(HIO_3)_2(HIO_2)_1(DMA)_2$	2	1	0	1
$(HIO_3)_1(HIO_2)_2(DMA)_1$	0	0	0	0
$(HIO_3)_1(HIO_2)_2(DMA)_2$	1	1	0	0
$(HIO_3)_3(HIO_2)_1(DMA)_1$	1	1	0	0
$(HIO_3)_1(HIO_2)_3(DMA)_1$	1	1	0	0
$(HIO_3)_2(HIO_2)_2(DMA)_1$	1	1	0	0

Section S5: References

He, X. C., Tham, Y. J., Dada, L., Wang, M. Y., Finkenzeller, H., Stolzenburg, D., Iyer, S., Simon, M., Kurten, A., Shen, J. L., Rorup, B., Rissanen, M., Schobesberger, S., Baalbaki, R., Wang, D. S., Koenig, T. K., Jokinen, T., Sarnela, N., Beck, L. J., Almeida, J., Amanatidis, S., Amorim, A., Ataei, F., Baccarini, A., Bertozzi, B., Bianchi, F., Brilke, S., Caudillo, L., Chen, D. X., Chiu, R., Chu, B. W., Dias, A., Ding, A. J., Dommen, J., Duplissy, J., El Haddad, I., Carracedo, L. G., Granzin, M., Hansel, A., Heinritzi, M., Hofbauer, V., Junninen, H., Kangasluoma, J., Kemppainen, D., Kim, C., Kong, W. M., Krechmer, J. E., Kvashin, A., Laitinen, T., Lamkaddam, H., Lee, C. P., Lehtipalo, K., Leiminger, M., Li, Z. J., Makhmutov, V., Manninen, H. E., Marie, G., Marten, R., Mathot, S., Mauldin, R. L., Mentler, B., Mohler, O., Muller, T., Nie, W., Onnela, A., Petaja, T., Pfeifer, J., Philippov, M., Ranjithkumar, A., Saiz-Lopez, A., Salma, I., Scholz, W., Schuchmann, S., Schulze, B., Steiner, G., Stozhkov, Y., Tauber, C., Tome, A., Thakur, R. C., Vaisanen, O., Vazquez-Pufleau, M., Wagner, A. C., Wang, Y. H., Weber, S. K., Winkler, P. M., Wu, Y. S., Xiao, M., Yan, C., Ye, Q., Ylisirnio, A., Zauner-Wieczorek, M., Zha, Q. Z., Zhou, P. T., Flagan, R. C., Curtius, J., Baltensperger, U., Kulmala, M., Kerminen, V. M., Kurten, T., Donahue, N. M., Volkamer, R., Kirkby, J., Worsnop, D. R., and Sipila, M.: Role of iodine oxoacids in atmospheric aerosol nucleation, Science, 371, 589-595, 10.1126/science.abe0298, 2021.

Liu, L., Li, S. N., Zu, H. T., and Zhang, X. H.: Unexpectedly significant stabilizing mechanism of iodous acid on iodic acid nucleation under different atmospheric conditions, Sci. Total Environ., 859, 159832, 10.1016/j.scitotenv.2022.159832, 2023.

Ning, A., Liu, L., Zhang, S. B., Yu, F. Q., Du, L., Ge, M. F., and Zhang, X. H.: The critical role of dimethylamine in the rapid formation of iodic acid particles in marine areas, NPJ Clim. Atmos. Sci., 5, 10.1038/s41612-022-00316-9, 2022.

Rong, H., Liu, J. R., Zhang, Y. J., Du, L., Zhang, X. H., and Li, Z. S.: Nucleation mechanisms of iodic acid in clean and polluted coastal regions, Chemosphere, 253, 10.1016/j.chemosphere.2020.126743, 2020.

Zhang, S. B., Li, S. N., Ning, A., Liu, L., and Zhang, X. H.: Iodous acid - a more efficient nucleation precursor than iodic acid, Phys. Chem. Chem. Phys., 24, 13651-13660, 10.1039/d2cp00302c, 2022.